Document downloaded from:

http://hdl.handle.net/10251/97089

This paper must be cited as:

J. Antonino-Daviu; Riera-Guasp, M.; José Roger-Folch; Martínez Jiménez, F.; Peris Manguillot, A. (2006). Application and Optimization of the Discrete Wavelet Transform for the Detection of Broken Rotor Bars in Induction Machines. Applied and Computational Harmonic Analysis. 21(2):268-279. doi:10.1016/j.acha.2005.12.003

The final publication is available at

http://doi.org/10.1016/j.acha.2005.12.003

Copyright Elsevier

Additional Information

Application and Optimization of the Discrete Wavelet Transform for the Detection of Broken Rotor Bars in Induction Machines

J. Antonino-Daviu* M.Riera-Guasp* J. Roger-Folch* F.Martínez-Jiménez** A.Peris-Manguillot**

* Universidad Politécnica de Valencia
Department of Electrical Engineering
P.O.Box 22012, 46071 Valencia, Spain
Phone: 0034963877592, Fax: 0034963877599

** Universidad Politécnica de Valencia
Department of Applied Mathemathica-IMPA-UPV
P.O.Box 22012, 46071 Valencia, Spain
Phone: 0034963877662, Fax: 0034963877660

ADDRESS FOR MANUSCRIPT CORRESPONDANCE:

Jose A. Antonino
Universidad Politécnica de Valencia
Dep. Electrical Engineering
P.O.Box 22012, 46071 Valencia, Spain
Phone: 0034-620384690, Fax: 0034963877599
e-mail: joanda@die.upv.es

ABSTRACT

The problem of the bar breakage diagnosis in electrical induction cage machines is a matter of increasing concern nowadays, due to the widely spread use of these machines in the industry. The classical approach, focused on the Fourier analysis of the steady-state current, has some drawbacks that could be avoided if a study of the transient behaviour of the machine is performed. The Discrete Wavelet Transform (DWT) is an ideal tool for this purpose, due to its suitability for the analysis of signals whose frequency spectrum is variable in time. The paper shows how the study of the high-level signals resulting from the DWT of the transient starting current of an induction motor allows the detection of a particular characteristic harmonic that occurs when a rotor bar breakage has taken place. This constitutes an alternative approach that avoids some problems that the traditional method implies and that can even lead to a wrong diagnosis of the fault. In the work, the application of the DWT for broken bar detection is optimized, regarding certain parameters of the transform such as type of the mother wavelet, number of decomposition levels, order of the mother wavelet and sampling frequency.

Keywords: Discrete Wavelet Transform, induction machines, fault diagnosis, rotor bar breakages, characteristic pattern

I. INTRODUCTION

The utilization of induction machines is widely spread in the industry due to its high reliability, low cost and appropriate characteristics for a great number of industrial applications. However, these machines can be affected by some faults which, if not early detected, can lead to a global failure and to the interruption of the process in which they are involved, with the subsequent economic losses.

Predictive maintenance of this electrical machinery has become a field of increasing significance during the last years because these machines often constitute critical parts of many industrial processes.

Among all the faults feasible to occur in induction machines, the rotor bar breakages constitute a non-negligible percentage as Thomson showed [1]. This can become a quite dangerous fault since, in the early stages, it often has not a clear reflect over the machine behaviour, leading to an abrupt collapse of the machine if the fault is not detected previously.

Many authors have developed during the last decades several methods in order to diagnose the presence of such a fault in induction machines. In this context, the classical approach for the detection of rotor bar breakages is focused on the application of the Fourier Transform to the stator current for the machine running in steady-state. The detection of the fault is done by studying two harmonic components that appear around the supply frequency component when a rotor bar breakage takes place. These components are known as sideband components (left and right) and their frequencies are given by (1), as shown by Deleroi [2].

$$f_b = (1 \pm 2 \cdot s) \cdot f \quad , \tag{1}$$

where f is the supply frequency and s is the slip: $s = \frac{n_s - n}{n_s}$; n_s is a constant (the synchronous speed) and n is the speed of the machine.

When a rotor bar breakage takes place, the amplitudes of these components are significantly increased, being feasible their use for the diagnosis of the breakage. This can be seen through comparison between Fig. 1 (a) and Fig. 1 (b), which show the spectra of a healthy machine and a machine with one broken bar, respectively. This classical approach has some important advantages such as the simplicity of the data acquisition systems and the required software, along with the robustness of the tool, which has hitherto provided quite satisfactory results. However, its validity has some drawbacks when the approach is applied under certain conditions. This is the case, for instance, of light-loaded or unloaded machines. In those situations, the slip *s* is very low and the sideband components practically overlap the supply frequency (Fig. 1 (c)). This makes difficult to detect their presence and to use them for the diagnosis, as Douglas remarked [3].

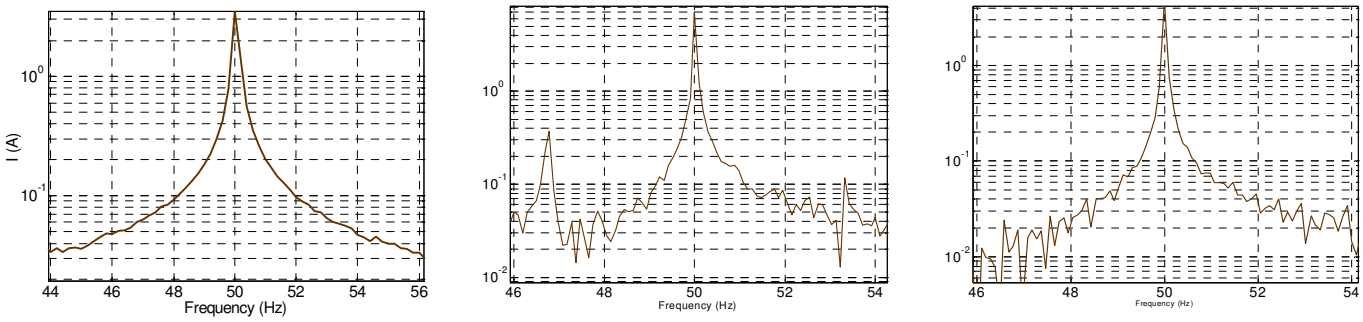

(a) **(b)** **(c)**

Figure 1. Classical detection of broken rotor bars. (a) loaded healthy machine, (b) loaded machine with one broken bar, (c) unloaded faulty machine

In addition, there are other phenomena, different to broken bars, such as ball bearing defects, voltage oscillations or load fluctuations that can cause the appearance in the steady-state current spectrum of similar frequencies to those associated with the sideband components. This is the case when the motor drives devices such as compressors, pumps and particularly mills and other machines with coupled gear reducers. It can be said that any external cause capable to provoke fluctuations in the speed of the motor or, equivalently, in its torque, can cause the appearance of harmonics in the supply currents, as Schoen

remarked [4]. If those harmonics have frequency values close to those of the sideband components, they can create confusion or even lead to a wrong diagnosis. Fig. 2 shows the similarity between the Fourier Transform of the steady-state current for a machine with two broken rotor bars (Fig. 2(a)) and for a healthy machine with a fluctuating torque load (Fig. 2 (b)).

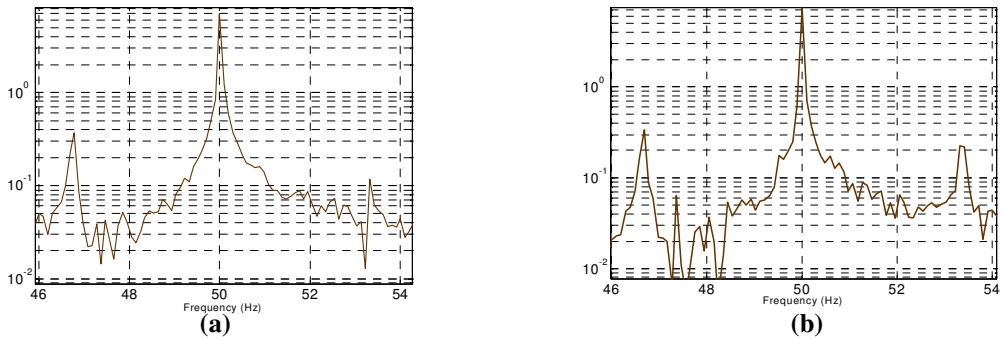

Figure 2. (a) Sideband components due to broken bars. (b) frequencies due to fluctuating torque in healthy machine

These and other disadvantages led many authors to focus their research on the study of the behaviour of the machine during the transient processes in order to develop new methods for the diagnosis of the fault. Some works were focused on studying the operation of the machine during the startup transient as those by Burnett [5] and Watson [6]. These works proposed the detection of the left sideband component, associated with broken rotor bars, during this transient as a way to indicate the presence of the breakage in the machine. They even proposed the convolution with a Gaussian wavelet in order to reveal the presence of this component. Recent works by Douglas [3] or Zhang [7] applied the wavelet transform to the startup current, although they were focused on the variations in particular parameters of this transform, such as the wavelet coefficients or the wavelet ridge.

A new method based on the application of the Discrete Wavelet Transform to the startup stator current was developed recently by the authors. It focuses on the study of the high-level wavelet signals resulting from the decomposition of the startup current during the transient, as a way to detect the presence of the

left sideband component. The energy of these signals shows a clear increase when a rotor bar breakage has taken place. In addition, their oscillations show a characteristic pattern that reveals the presence of the component during the transient, since that pattern fits exactly with the frequency variation of the left sideband, as it will be shown in Section IV. Thus, the diagnosis using those signals is based on a direct interpretation of the physical phenomenon that is taking place.

An important advantage of this method is that it leads to a correct diagnosis in some cases in which the classical approach does not provide so accurate results, such as unloaded machines or machines with fluctuating torque load. This was proven in several experiments developed in industrial machines.

Moreover, the wavelet signals (approximation and high-order details) resulting from the DWT act as filters, according to the Mallat algorithm, allowing the automatic extraction of the time evolution of the low frequency components that are present in the signal during the transient. The computation time required for the analysis is usually negligible and, at the same time, the proposal avoids the need of intricate algorithms for the extraction of the evolution of the signal components. This makes this method suitable for its incorporation in portable condition monitoring devices which allow the on-line diagnosis of the breakage in industrial machinery (Fig. 3).

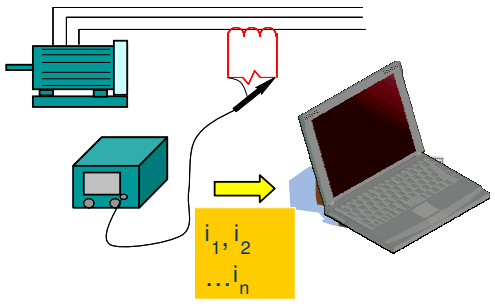

Figure 3. Portable equipment for broken bar detection

The scheme of the method presented in this paper can be extended for the diagnosis of other types of faults in electrical machines, such as eccentricity, inter-turn or inter-coil short-circuit or ball-bearings

defects, or even could be applied to any kind of system, in which a fault produces harmonics with a characteristic evolution along transient regimes.

II. THE PHYSICAL PHENOMENON

The startup transient of an induction motor comprises the period after it is switched on. During that period, the machine accelerates from the standstill to the rated speed. In a healthy induction machine, the startup current is an amplitude-changing, 50 Hz (supply frequency) sinusoidal signal $i(t)$ given by (2), where $\hat{I}(t)$ is the RMS value of the current. This signal, obtained for a specific machine, is plotted in Fig. 4.

$$i(t) = \sqrt{2} \cdot \hat{I}(t) \cdot sen\ 2 \cdot \pi \cdot 50 \cdot t \tag{2}$$

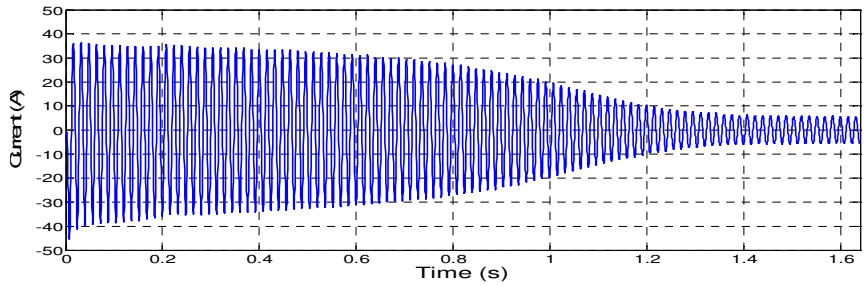

Figure 4. Startup current in a stator phase for a healthy machine

When a rotor bar breakage takes place, a distortion occurs in the air-gap field. This distortion induces several frequency components in the stator current spectrum as Deleroi remarked [2]. In steady-state, the frequencies of these components depend on the speed of the machine; Among these components, the most important used for the diagnosis of broken rotor bars in induction machines is that known as *left sideband harmonic*, whose frequency is given by (3).

$$f_{Ls} = f \cdot |(1-2 \cdot s)| \tag{3}$$

During the startup transient that harmonic evolutes. In Fig. 5 (c) is plotted this evolution, calculated for a simulated startup transient. This component can be roughly described as a sinusoidal wave, the frequency of which changes continuously during the startup, as the slip (or speed) changes. Fig. 5 (a) and (b) show the variation of the speed and frequency of left sideband during the startup, respectively. The frequency decreases from a value equal to the supply frequency (f=50 Hz) when the machine is connected, and reaches 0 Hz, when the rotor speed is half the synchronous speed (s=0.5). From this on, it increases again to reach a value close to the supply frequency, when the steady-state regime is reached.

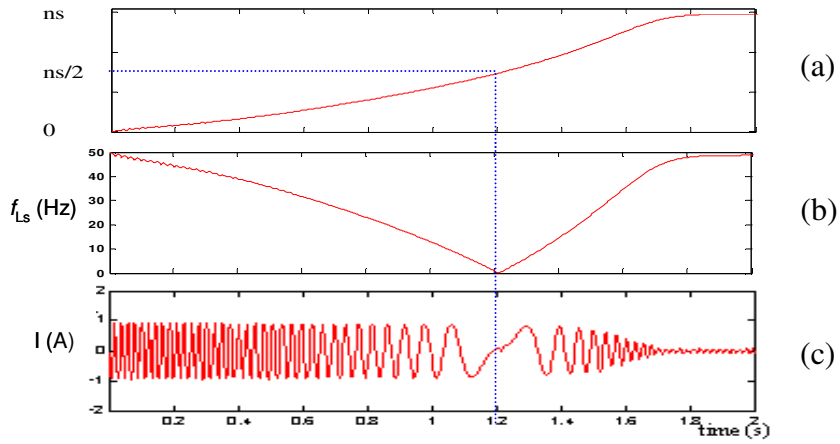

Figure 5. Evolution during the transient of: (a) the speed of the machine (b) the frequency of the left sideband component (c) the left sideband component

Since the amplitude of the left sideband component is usually much greater than those of the rest of the components that appear due to the breakage, the startup current for a machine with a broken bar can be approximated by the addition of the startup current for the machine in healthy state plus the left sideband harmonic evolution (Fig. 6). However, due to the low amplitude of the sideband harmonic with respect to the current, it is not feasible to distinguish directly between the current for a faulty machine and that for a healthy one. Two equivalent methods based on the application of the Discrete Wavelet Transform (DWT) to the startup transient current will be applied for extracting the sideband harmonic during the startup and allowing the diagnosis of the bar breakage.

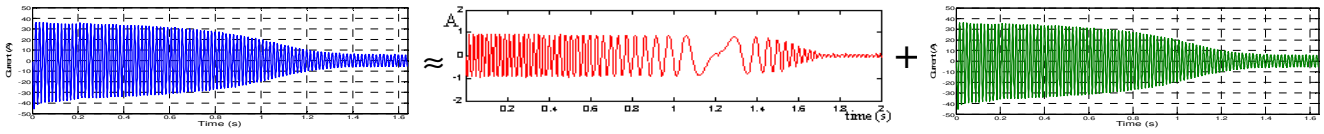

(a) **(b)** **(c)**

Figure 6. (a) Startup current for a machine with one broken rotor bar. (b) Left sideband component (c) Startup current for a machine in healthy state

III. THE PROPOSED METHOD

A) First approach: Analysis based on the pattern of the high level DWT signals.

The first approach is focused on the analysis of the high-level detail (and approximation) signals resulting from the wavelet decomposition, whose associated frequency bands are included within the interval that extends from 0 to almost the supply frequency. Fig. 7 compares the DWT of the startup current in the cases of healthy machine (Fig.7 (a)) and faulty machine (Fig. 7 (b)). For the faulty machine it can be seen how the variations of the high level signals *d6* , *d7* and *a7* are arranged according with the evolution of the left sideband harmonic frequency, plotted in Figure 6 (b); first, there is an increment in the energy of *d6* (frequency band [12.8 , 25.6 Hz]). Next, the energy increment appears in d_7 (frequency band [6.4, 12.8 Hz]) and then in *a7* (frequency band [0, 6.4 Hz]). After that, the oscillations appear again in d_7 and finally in d_6. This characteristic pattern of the high-level signals *d6*, *d7* and *a7* in the startup current allows for a reliable diagnosis of the bar breakage.

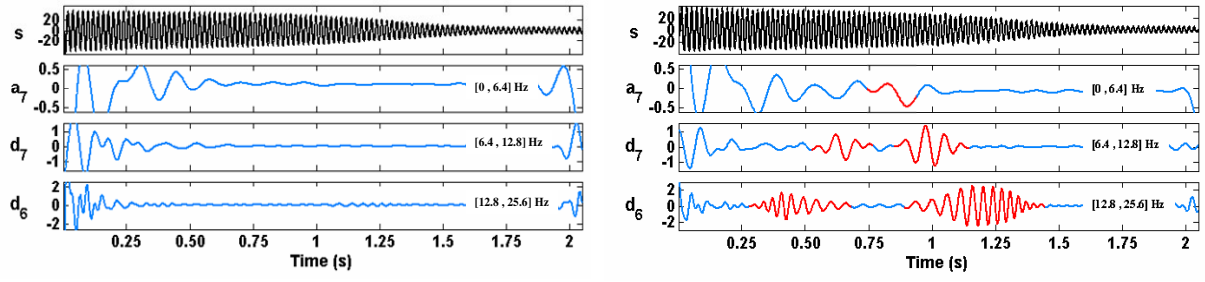

(a) (b)

Figure 7. (a) High-level wavelet signals resulting from the DWT of the tested startup current for a: (a) healthy machine (b) machine with 2 broken rotor bars

B) Second approach: Analysis based on the shape of the approximation signal

Since according to wavelet theory, the approximation signal at level *n* is the aggregation of the approximation at level *n*-1 plus the detail at level *n*-1 (MRA algorithm), it is needed only one signal to reflect the whole evolution of the left sideband component. This signal is the approximation signal whose associated frequency band extends from 0 to near *f*, being *f* the supply frequency. The second proposed approach is based on the study of this signal, as a way to extract the evolution of the harmonic and, thus, to diagnose and quantify the presence of breakages. Fig. 8 shows this signal, obtained from simulations for a healthy machine (Fig. 8 (a)) and for a machine with two broken bars (Fig. 8 (b)). As it is seen, the approximation signal does not show any variation for the first case, because the machine does not have any bar breakage and, thus, the magnitude of the sideband component is negligible. On the other hand, when there are broken bars, that signal shows an evolution that practically fits with the evolution of the sideband component during the startup (Fig. 8 (b)). It can be seen how the frequency of this signal decreases to zero and then increases again.

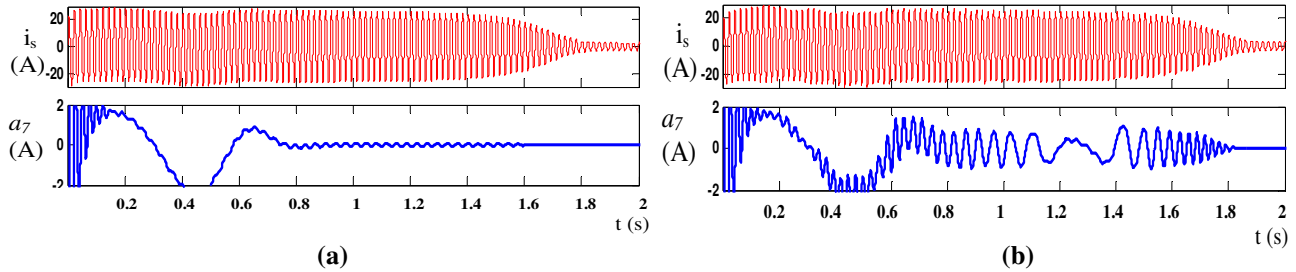

Figure 8. Simulated startup currents (up) and level 7 approximation signals (down) in the case of healthy machine (a) and faulty machine (b).

Rigorously speaking, this signal does not reflect completely the evolution of the harmonic, since its frequency band does not extend until the supply frequency but near this frequency. This is due to the non-ideality characteristic of the wavelet filtering, which causes the overlapping between bands and makes

advisable not to extend the band very near the supply frequency in order to avoid this component to mask the harmonics within the adjacent bands. This aspect will be emphasized later.

IV. EXPERIMENTAL RESULTS

For the validation of the method, several tests were performed with a set of 4-pole 1.1 kW industrial induction motors. The rotor bar breakages were forced in the laboratory, opening the motors and drilling artificially the holes in the different bars (Fig. 9 (b)). The main characteristics of the tested motors were: Star connection, rated voltage (U_n): 400V, rated power (P_n): 1.1 kW, 2 pair of poles, primary rated current (I_{1n}): 2.7A, rated speed (n_n): 1410 rpm and rated slip (s_n): 0.06. The number of rotor bars is 28.

Each motor was coupled to its load through a system of pulleys in order to couple both machines through different speed rates. Fig. 9 (a) shows the experimental setup. The load was a DC machine with rated speed 2000-3000 rpm, rated voltage 220 V, 3 kW, 1 pair of poles, excitation rated current: 0.4 A, armature rated current: 13.6 A. The supply frequency used in the experiments was 50 Hz.

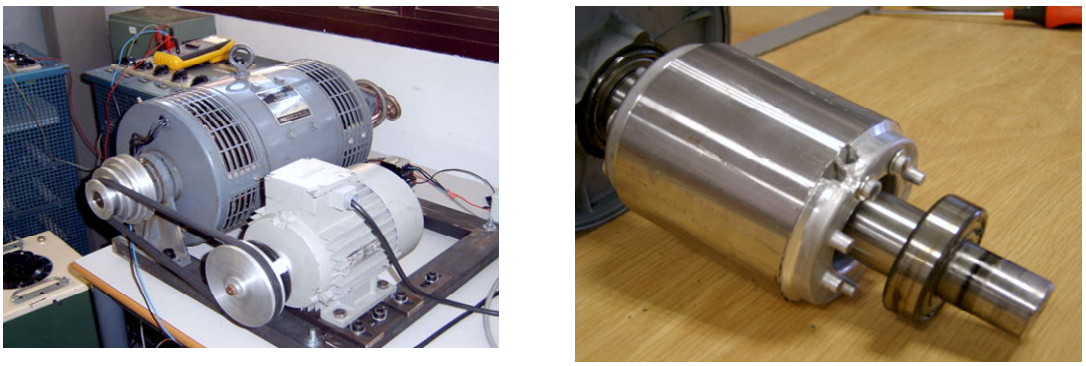

(a) (b)

Figure 9. (a) Experimental setup for 1.1 kW motors tests (b) Bar breakages in the induction motor rotor

The primary current was measured during the startup transient and in steady-state for the different cases tested. The sampling frequency used for capturing the signals was 5000 samples/sec. The DWT of the startup current was performed using the MATLAB Wavelet Toolbox. 8-level and 6-level decomposition

was performed in order to obtain the results using the two above commented approaches. Daubechies-44 mother wavelet was used for the analysis. Table I shows the frequency bands corresponding to the high-order wavelet signals resulting from the analysis, according to the sampling rate used for the tests.

TABLE I. FREQUENCY BANDS FOR THE HIGH-LEVEL WAVELET SIGNALS

8-level decomposition		**6-level decomposition**	
Level	Frequency band	Level	Frequency band
d6	39.06 – 78.12 Hz	*d6*	39.06 – 78.12 Hz
d7	19.53 – 39.06 Hz	*a6*	0 – 39.06 Hz
d8	9.76 – 19.53 Hz		
a8	0 – 9.76 Hz		

The cases that were considered are:

A) Healthy machine under full load

Fig. 10 (a) shows the 8-level DWT of the startup current. It can be seen that the upper-level signals (*a8*, *d8* and *d7*), associated with frequency bands below 50 Hz, do not show any significant variation, apart from the initial oscillations that last only few cycles. Fig. 10 (b) shows the approximation signal arising from the 6-level DWT (*a6*). No important oscillations appear in that signal. From both approaches it can be concluded that the left sideband component, associated with broken bars, is not present.

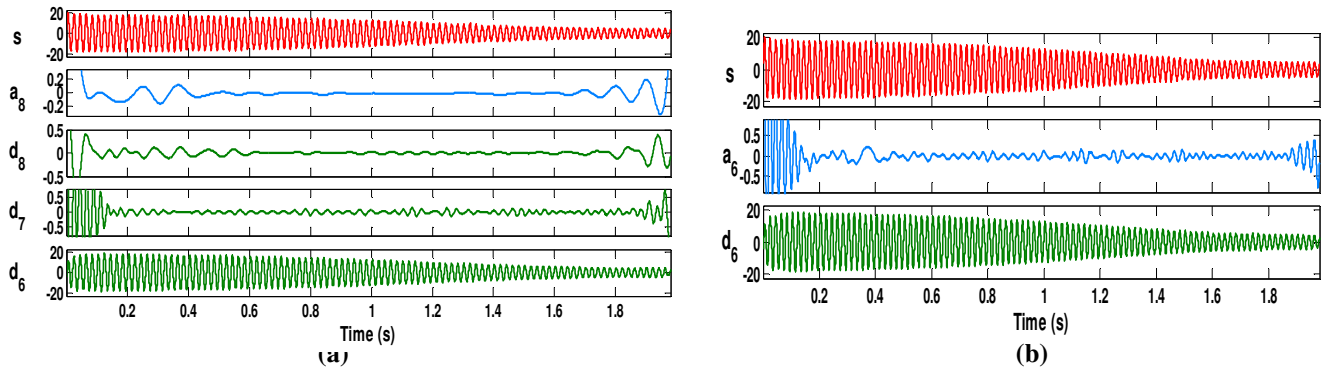

Figure 10. Healthy machine; (a) 8-level DWT of the startup current (b) 6-level DWT of the startup current

B) Loaded machine with two broken rotor bars

Fig. 11 displays the DWT analysis of the current. As shown in Fig. 11 (a), a significant increase with respect to the healthy state appears in the energy of the high-level signals (*a8*, *d8* and *d7*). The oscillations

in those signals are due to the evolution of the left sideband component during the transient. These oscillations follow a sequence that is according to the frequency evolution of the left sideband component commented above. Fig. 11 (b) shows the approximation signal resulting from the 6-level decomposition. Since this signal reflects approximately the evolution in amplitude and frequency of the left sideband component, its energy shows a clear increase with respect to the healthy state. The oscillations that appear at the beginning, that mask slightly the evolution of the harmonic, are caused by the electromagnetic transient of the machine and to the border effect of the wavelet transform and they also appear in the healthy state as shown above. The masking produced by these oscillations can become especially important if the startup is very fast.

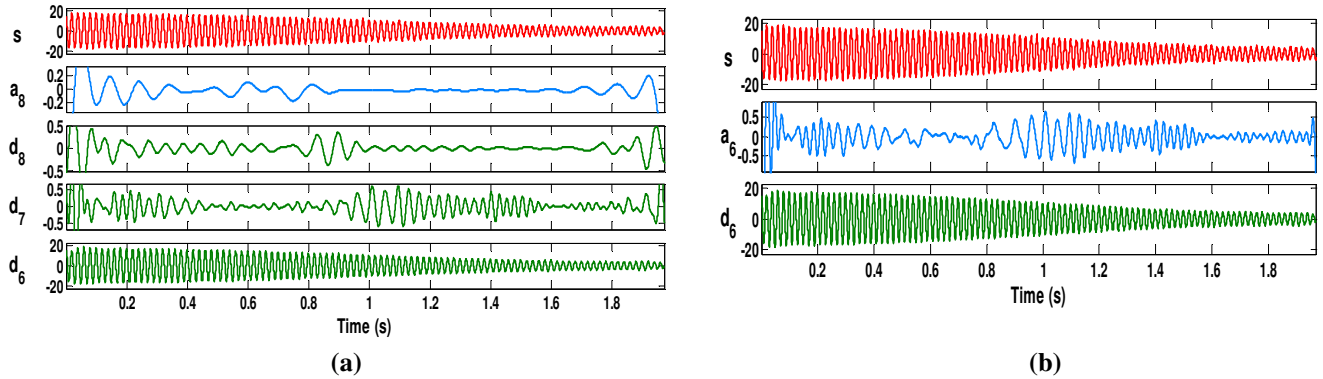

(a) **(b)**

Figure 11. Machine with 2 broken bars; (a) 8-level DWT of the startup current (b) 6-level DWT of the startup current

C) Unloaded machine with two broken rotor bars

In this case, the application of the classical method, based on Fourier analysis, is not valid, since the slip is very low and the sideband components overlap the supply frequency component. This makes very difficult the diagnosis of the fault. Nevertheless, the high-order wavelet signals (*a8*, *d8* and *d*7) resulting from the DWT analysis of the startup current show a clear increase in their energy, if compared with the healthy state. In addition, their oscillations fit well with the left sideband frequency evolution described above. Furthermore, the approximation signal also shows clear variations (Fig. 12 (b)), reflecting the

evolution of the sideband component. This leads to the conclusion that a bar breakage is present on the machine. This case is an example of the validity of the approach in a case when the classical method is not suitable to be applied.

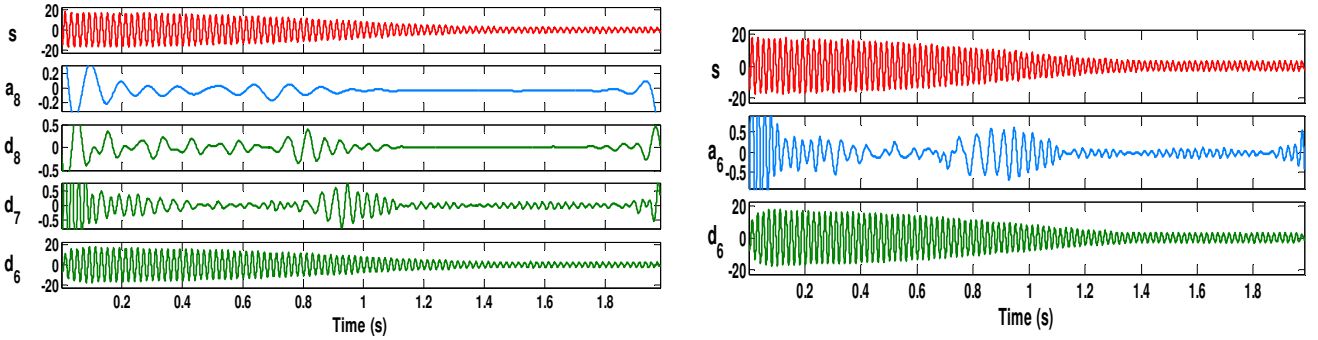

Figure 12. Unloaded machine with 2 broken bars; (a) 8-level DWT of the startup current (b) 6-level DWT of the startup current

D) Healthy machine under full load with periodical fluctuation in the supply voltage

In this case, the machine is healthy, but it works under a voltage system whose RMS value fluctuates periodically. This situation can take place, for instance, in machines supplied by low short-circuit power networks that feed at the same time other devices which consume energy in an oscillating way.

The spectrum obtained if applying the FFT is quite similar to the one corresponding to the loaded machine with 2 broken rotor bars. This was shown in Fig. 2. Thus, the application of the classical approach could provide a wrong diagnosis of the rotor breakage. On the other hand, the oscillations in the signals obtained with the DWT (Fig 13 (a)) do not fit with the rotor bar breakage pattern. In addition, the oscillations in the approximation signal (Fig. 13 (b) are not very high and do not fit with the shape of this signal for a machine with broken bars, shown above. These facts allow discarding the existence of this fault. In this example, the proposed method behaves correctly, whereas the Fourier approach can lead to erroneous conclusions.

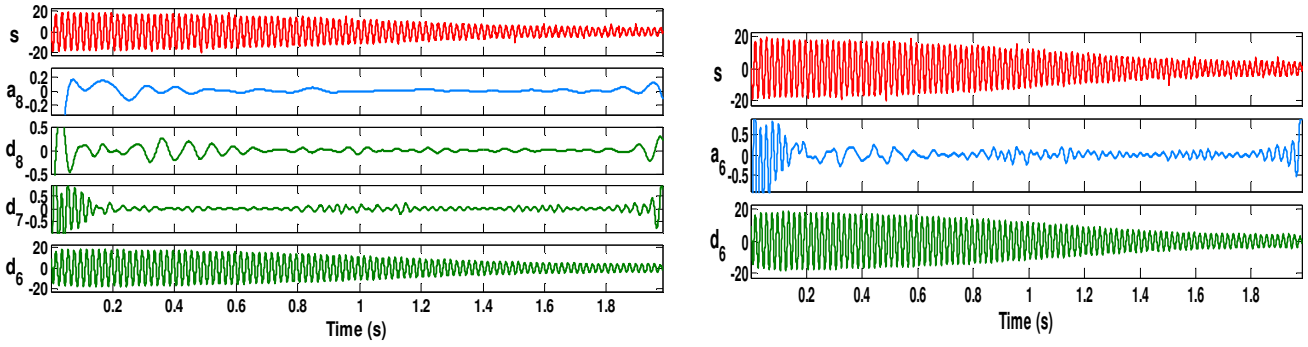

(a) (b)

Figure 13. Healthy machine under full load with periodical fluctuation in the supply voltage; (a) 8-level DWT of the startup current (b) 6-level DWT of the startup current

V. OPTIMIZATION OF THE DWT PARAMETERS

The tests developed with different laboratory machines and commercial motors showed the validity of the results. However, for the application of both methods, some wavelet parameters have to be fixed. Among these parameters should be remarked the sampling frequency, the type of mother wavelet, the order of the mother wavelet and the number of levels for the decomposition.

1. Sampling frequency

According to Nyquist criteria, for extracting a certain frequency from a signal, it has to be sampled with a minimum sampling frequency, at least twice the maximum frequency to be detected. On the other hand, the Mallat decomposition algorithm involves a relation between the wavelet signals resulting from the decomposition (approximation and details) and the frequency bands associated with those signals as it was seen above. Considering these two facts, the minimum sampling frequency that is needed to obtain an approximation signal with an upper limit of its associated frequency band equal to the supply frequency, f, is $f_s=4 \cdot f$. Therefore, this is the minimum sampling frequency for applying any of the two above commented approaches, since, if the first approach is wanted to be applied, it is only necessary to decompose this approximation signal, this is, to consider more levels. Greater sampling frequencies imply

the use of more decomposition levels to get such an approximation signal. Nevertheless, these low-level signals contain no useful information for the application of the method, since their associated frequencies are higher than the range in which the sideband evolutes.

Fig. 14 (a) and (b) show the DWT decomposition using a sampling frequency of 312 samples/second and 625 samples/second respectively. The approximation signal, in these cases, includes frequencies in the range [0-39] Hz. Higher sampling frequencies imply more decomposition levels, although they are not useful for the analysis of the phenomenon.

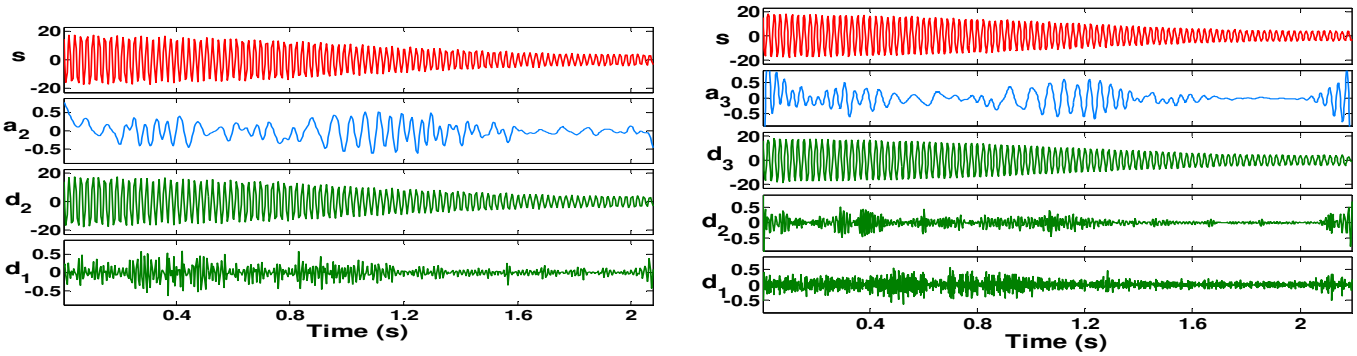

Figure 14. DWT for a current signal with: (a) sampling frequency f_s=312 samples/second and (b) f_s=625 samples/s.

2. Type of mother wavelet

DWT decompositions of the startup current were performed using several types of mother wavelets (Daubechies, coiflet, simlet, biorthogonal and discrete Meyer (dmeyer) wavelet were considered in the analysis). Despite the different properties of those families, the qualitative analysis of the results showed that no sensible advantages appeared when selecting a specific wavelet family, since the patterns that arose in the high-level signals when a bar breakage was present in the machine were quite similar. In addition, the computation of the energy of those high-level signals per unit energy of the original current signal showed also high similarities. Finally, due to the well-known properties of the orthogonal

Daubechies family, it was decided to use a mother wavelet of this family, despite its non-optimal frequency response, a fact that creates some problems which will be commented later.

As an example of all these considerations, Fig. 15 shows the high-level wavelet signals, resulting from the DWT decomposition of the startup current for a machine with 2 broken bars. In Fig. 15 (a) is used db-44 as mother wavelet whereas in Fig. 15 (b) is used dmeyer. Despite these wavelets have very different properties, the patterns resulting from the application of the method are quite similar, as it is observed in that figure, where the application of the first approach is shown.

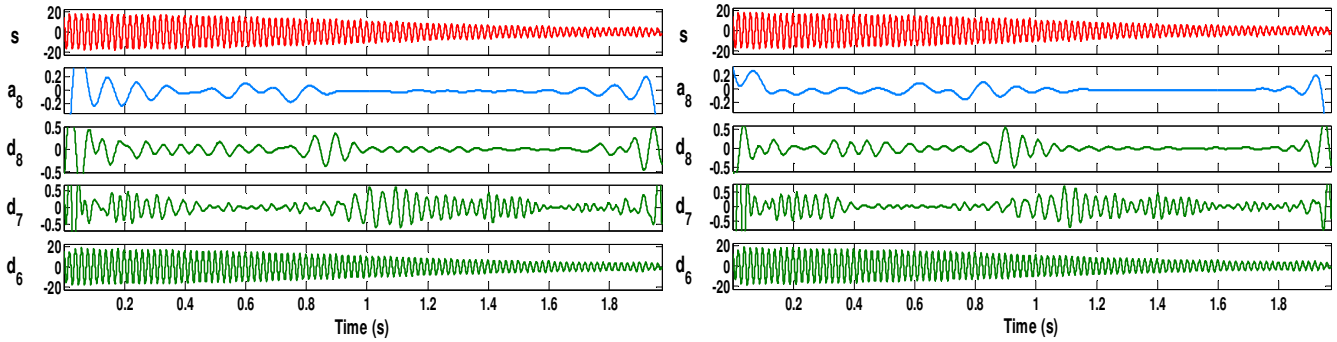

Figure 15. 8-level DWT decomposition for a current signal using as mother wavelet: (a) daubechies-44 (b) dmeyer

3. *Order of the mother wavelet*

Wavelets are far from behaving as ideal filters. The presence of a transition bandwidth whose width is non-negligible and the ripple inherent to the filters cause the partial overlapping between frequency bands, arising the problem of shift-variance. As Chui showed [8], filter characteristics of the Daubechies scaling functions and wavelets improve significantly when higher is the order of the wavelet. This is shown through the side-lobe/main-lobe power ratios and the maxima side-lobe/main-lobe ratios of the filter characteristics of the scaling and wavelet functions at the different levels. These ratios are lower when higher is the order of the considered wavelet, giving an idea of the ideal characteristic of the filter.

Thus, when using classical Daubechies wavelets for the application of the method, a possible way to reduce the influence of the overlapping between bands is to select a high-order mother wavelet. Then, more ideal will be the behaviour of the filter and less important will be the effect of overlapping between frequency bands. This is shown in Fig. 16, where DWT decomposition is performed using db-10 and db-44. When db10 is used, the main component of the current, which is contained within the detail d6 overlaps the adjacent signal d7, hiding the characteristic evolution of the sideband within this signal. This problem is minimized when using db44 as it can be seen in Fig 16 (b). However, due to larger length of the associated filter, there will be an increment of the computational requirements in this case.

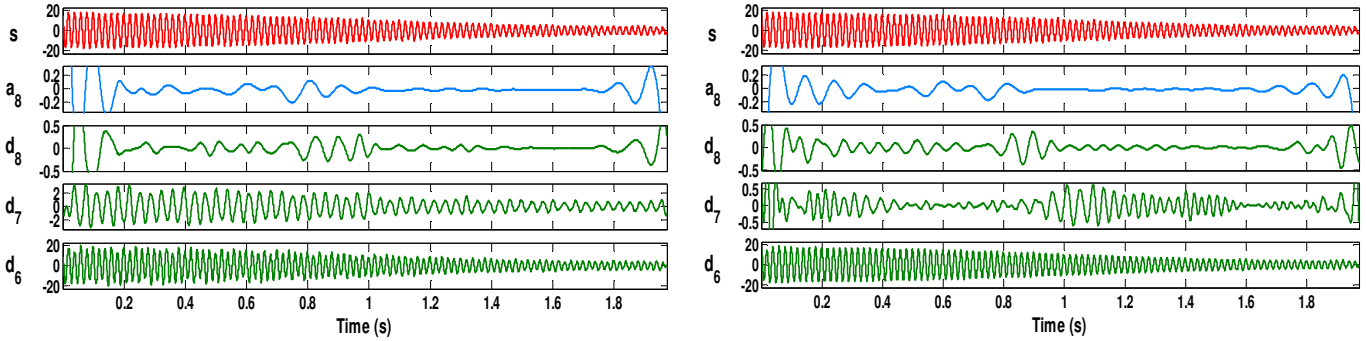

Figure 16. DWT of the startup current for a machine with 2 broken bars using; (a) db 10 (b) db44

Several solutions have been proposed during these last years for solving the problem of overlapping between bands and improve the frequency response of the wavelet filtering. As Chui proved [8], use of appropriate biorthogonal spline wavelets constitutes a possible solution, since the ripple effect and the transition bandwidths are substantially decreased. Side-lobe/main-lobe power ratios of the frequency response of this type of wavelets improve those of the Daubechies family. Other authors, proposed the use of the Continuous wavelet Transform (CWT) although, in this case there is a tradeoff between less shift variance and higher computational requirements of CWT, as Bradley stated [9]. Other works have been done regarding the design of suitable frequency response wavelets for signal representation [10].

4. Number of levels of decomposition

The suitable number of levels of decomposition (n_{Ls}) depends on the sampling frequency of the signal being analysed (f_s). For each one of the proposed approaches, it has to be chosen in order to allow the high-level signals (approximation and details) to cover all the range of frequencies along which the sideband component varies during the startup (that is, 0 Hz to near the fundamental frequency *f*).

From condition (4) it can be calculated the minimum number of decomposition levels that it is necessary for obtaining an approximation signal (a_{nf}) so that the upper limit of its associated frequency band is under the fundamental frequency:

$$2^{-(n_f+1)} \cdot f_s < f \tag{4}$$

From this, the decomposition level of the approximation signal which includes the left sideband harmonic, is the integer n_{Ls} given by (5).

$$n_{Ls} = \mathrm{int}\left(\frac{\log(f_s / f)}{\log(2)} - 1\right) \tag{5}$$

This would be the necessary number of levels for applying the second proposed approach, based on the approximation signal. For the first approach, further decomposition of this signal would have to be done, so that the frequency band [0-*f*] would be decomposed in more bands. Usually, two more decomposition levels (that is, $n_{Ls} + 2$) would be adequate for the analysis.

VI. CONCLUSIONS

In this work two physically based applications of the DWT for the diagnosis of rotor bar faults in induction cage motors are presented, validated and optimized. The diagnosis is based on the analysis of the high level signals obtained from the DWT of the startup current signal. The first approach is focused

on the study of the high-level approximation and detail signals that contain the time evolution of frequencies below the supply frequency. These signals allow the detection of the frequency evolution of a characteristic harmonic associated with the breakage during the startup transient. The second approach is based on the study of the approximation signal, aggregation of those signals considered in the previous approach. That signal shows the evolution, in amplitude and frequency of the harmonic associated with the fault during the transient.

Both approaches are tested experimentally in several cases. Results show the validity of both methods to detect the presence of the breakage in an induction machine, even in some cases in which the application of the classical approach, based on the Fourier transform of the steady-state current, cannot be applied or can lead to confusion or to a wrong diagnosis.

Furthermore, the application of the DWT is optimized, regarding the selection of some parameters such as sampling frequency, type of mother wavelet, order of the mother wavelet or number of levels of decomposition. The influence of these parameters over the results is analysed.

The proposed schemes, based on the DWT signals analysis, can be extended for diagnosis and discrimination among other types of faults in electrical machinery.

ACKNOWLEDGMENTS

The authors thank Professor C.K. Chui for his valuable comments and suggestions. We also thank the 'Vicerrectorado de Investigacion y Desarrollo' of 'Universidad Politecnica de Valencia' for financing and supporting part of this research.

REFERENCES

[1] W.T. Thomson, M. Fenger, *"Current signature analysis to detect induction motor faults",* IEEE Industry Applications Magazine, July/August 2001, pp. 26-34.

[2] W. Deleroi, *"Der stabbruch im kaufiglaufer eines asychonomotor",* Archiv fur Elektrotechnik, Vol. 67, 1984, pp. 91-99.

[3] H. Douglas, P. Pillay and A. Ziarani , *"Broken rotor bar detection in induction machines with transient operating speeds'*, IEEE Transactions on Energy Conversion, Vol. 20, No. 1, March 2005, pp. 135-141.

[4] R.R. Schoen, T.G. Habetler. "Evaluation and Implementation of a System to Eliminate Arbitrary Load Effects in Current-Based Monitoring of Induction Machines." *IEEE Transactions on Industry Applications,* Vol. 33, No. 6, November/December 1997, pp. 1571-1577.

[5] R. Burnett, J.F. Watson and S. Elder, *"The application of modern signal processing techniques to rotor fault detection and location within three phase induction motors"*, European Signal Processing Journal, Vol. 49, 1996, pp. 426-431.

[6] J.F. Watson and N.C. Paterson, *"Improved techniques for rotor fault detection in three-phase induction motors,"* in Proc. IEEE Industrial Applications, Vol. 1, 1998, pp. 271-277.

[7] Z. Zhang and Z. Ren, "A novel detection method of motor broken rotor bars based on wavelet ridge", *IEEE Transactions on Energy Conversion*, Vol. 18, No. 3, September 2003, pp. 417-423.

[8] C. K. Chui, *"Wavelets: A Mathematical Tool for Signal Analysis"*, SIAM, 1997.

[9] A.P. Bradley and W.J. Wilson, "*On wavelet Analysis of Auditory evoked Potentials,*" Clinical neurophysiology (Elsevier) 115, 2004, pp. 1114-1128.

[10] J.K. Zhang , T.N. Davidson and K. M. Wong, *"Efficient Design of Orthonormal Wavelet Bases for Signal Representation"*, IEEE Transactions on Signal Processing, Vol. 52, No. 7 , July 2004, pp. 1983-1996.